World Academy of Science, Engineering and Technology
International Journal of Civil and Environmental Engineering
Vol:17, No:2, 2023

Temperature-Based Detection of Initial Yielding Point in Loading of Tensile Specimens Made of Structural Steel

Aqsa Jamil, Hiroshi Tamura, Hiroshi Katsuchi, Jiaqi Wang

Abstract**—**Yield point represents the upper limit of forces which can be applied on a specimen without causing any permanent deformation. After yielding, the behavior of specimen suddenly changes including the possibility of cracking or buckling. So, the accumulation of damage or type of fracture changes depending on this condition. As it is difficult to accurately detect yield points of the several stress concentration points in structural steel specimens, an effort has been made in this research work to develop a convenient technique using thermography (temperature-based detection) during tensile tests for the precise detection of yield point initiation. To verify the applicability of thermography camera, tests were conducted under different loading conditions and measuring the deformation by installing various strain gauges and monitoring the surface temperature with the help of thermography camera. The yield point of specimens was estimated by the help of temperature dip which occurs due to the thermoelastic effect during the plastic deformation. The scattering of the data has been checked by performing repeatability analysis. The effect of temperature imperfection and light source has been checked by carrying out the tests at daytime as well as midnight and by calculating the signal to noise ratio (SNR) of the noised data from the infrared thermography camera, it can be concluded that the camera is independent of testing time and the presence of a visible light source. Furthermore, a fully coupled thermal-stress analysis has been performed by using Abaqus/Standard exact implementation technique to validate the temperature profiles obtained from the thermography camera and to check the feasibility of numerical simulation for the prediction of results extracted with the help of thermographic technique.

Keywords**—**Signal to noise ratio, thermoelastic effect, thermography, yield point.

I. Introduction

THE mechanical behavior of structural members and engineering materials is generally discussed by two important parameters, stress and strain. To determine the yield point of a specific specimen, mostly the stress is plotted against the strain. Previously, during the deformation process of a specimen, the variation of temperature is generally disregarded. This research focuses to detect the yield point by using the basic principle of thermoelastic effect and the comparison of results with the traditional method of determining yield point by utilizing the proof stress method just for validation purposes.

According to Hill [1], the yield point in structural steels can be defined as the instant when the plastic deformation first becomes possible as the load is increased. It represents the upper limit of forces that can be applied on a specimen without causing any permanent deformation. When a specimen is subjected to loading, elastic limit is the moment when there will be initial plastic localization, while yield point can be defined as the instant when the specimen first begins to deform plastically. It is essential to understand that elastic limit and yield point are two different aspects. When both are not synchronized, the body will behave completely as a rigid object at the respective loading interval [1].

For the uniaxial tensile loading test, yielding initiation is based on three criteria which are characterized as the limit of elasticity, limit of proportionality, and the yield point. According to Burczyński et. al., [2] the limit of elasticity is defined as the highest value of stress applied that can be resisted by material without any measured value of irreversible deformation. A constant incremental procedure of loading and unloading is required to determine the limit of elasticity. Due to this reason, it is sometimes replaced as the limit of proportionality defined as the greatest value of applied stress that holds a directly proportional relationship to the strain value. Finally, the yield point is defined as the stress at which an irreversible (plastic) strain value equal to 0.2% can be obtained [2]. The present study introduced an efficient method of yield point identification with the help of infrared thermography technique, which detects the temperature increase in steel (owing to its elasto-plastic nature) associated with the application of loading on the specimen due to the plastic deformation.

In thermography, by utilizing infrared (IR) radiations emanated from the object an IR thermographic camera encapsulates and makes the image of the specimen. IR radiations are converted into electrical signals and exhibited on a monitor in the form of a colored image in which various colors indicate different temperature levels. The energy rate emitted in the form of thermal radiations strongly depends on the object's surface temperature [3]. The first thermography camera was developed in 1929 by a great scientist named Kalman Tihanyi. In the past years, this invention made revolutionary development in the field of medical sciences [4], [5]. For the assessment of damage and investigations related to structural health conditions, thermal images provided by a thermographic camera proves to be an excellent tool [6], [7]. In the field of

Aqsa Jamil is PhD Candidate, Yokohama National University, 240-8501, 79-1 Tokiwadai, Hodogaya Ward, Yokohama, Japan (phone: +81-80-7243-1110; e-mail: jamil-aqsa-zf@ynu.jp).

Hiroshi Tamura, Associate Professor, Hiroshi Katsuchi, Professor, and Jiaqi Wang, Assistant Professor, are with Yokohama National University, Japan.

engineering and material science, the thermographic technique works on the fundamental concept of thermomechanical coupling i.e., evolution of temperature due to deformation of material by applying the load which was first studied by Lord Kelvin in 1853 [8]. This concept was further enhanced by [9] by introducing the dissipation function in terms of entropy along with the thermoelastic potential. Reference [10] proposed a method to evaluate the plastic deformation phenomena in a steel specimen by using the thermal video system (TVS-2100) and developed the surface temperature distribution of the specimen by changing its strain rate. By changing the strain rate, the size of plastic zone is affected, consequently altering the strength and overall fracture pattern of the specimen [11].

The standard method of tensile testing has been employed along with the thermography technique to study the deformation pattern and the associated heat generation for different kinds of materials. The rise of maximum temperature depends on the type of material, conditions in which tests were performed and the deformation pattern showed by respective material during the loading process. The non-destructive (NDE) thermography technique proved to be a potential tool for the recognition of thermal gradients and the plastic strain distribution by applying various loading rates. Visualization of failure and the deformation area, strain localization position and time, amount of dissipated heat energy, degree of change in the internal energy, identification of various stages can only be possible with the help of the IR thermography method [12]-[15].

In this study, a NDE method called the IR thermography technology, which entails no direct contact with the specimen and acquires thorough temperature mapping has been employed to stipulate the determination of yield point during the tensile testing of structural steel specimens. The method is based on the concept of thermomechanical coupling due to the force applied during the uniaxial tension test. For yield point detection, the concept of thermoelastic effect has been employed throughout this research work which explains that the stressing is isentropic (occurring at constant entropy and is reversible in nature) process in the range of elastic stress applied to the tensile specimen. The temperature profile from thermograms obtained through thermography camera was also validated by using fully coupled thermal stress numerical analysis performed using Abaqus.

II. Methodology and Description

This research work has been divided into two major parts: Laboratory testing and numerical simulation. In laboratory testing, uniaxial tensile testing of specimens has been performed and the deformation was measured by installing various strain gauges and monitoring the surface temperature with the help of a thermography camera. The stress-strain behavior and the temperature profiles are then superimposed to study the relationship between deformation and temperature behavior. In the second fold, alongside the experimentation, the simulations have been carried out using fully coupled temperature displacement analysis in Abaqus.

A. Experimental Setup

The complete experimental setup has been shown in Fig. 1, which includes the testing machine and an IR thermography camera. Three strain gauges have been attached to the coupon specimen for the validation of the camera. Using data acquisition system, data from the camera and strain gauges were transferred directly to the computers by using the real-time image transfer and LabVIEW respectively.

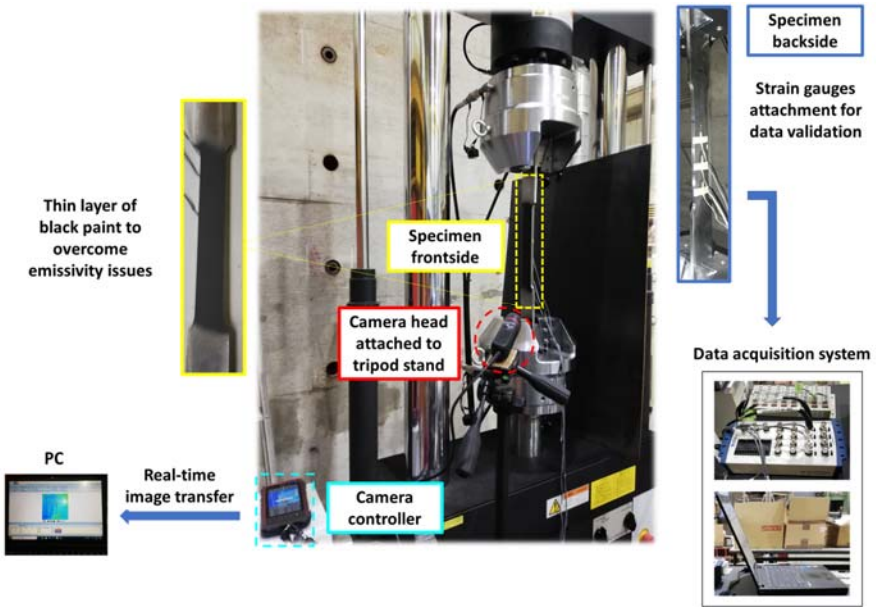

Fig. 1 Experimental configuration

B. Testing Specimen

The compact coupon specimens were prepared by using a material grade of SM400A according to the specifications of JIS G3106 standard. Fig. 2 shows the dimensions and geometry

of the tested specimens with overall length of 600 mm and gauge width of 40 mm. Several coupon specimens of the same geometry and chemical composition were employed in this study to make a better understanding for different purposes like repeatability analysis, disturbance effect due to temperature and light imperfections.

C. IR Thermography Camera

The thermograms were recorded with the help of "Thermo FLEX F50", a handy type of IR thermography camera introducing a concept of "Freestyle" in which the mechanism for attaching/detaching and rotating the camera head was equipped. By detaching the camera head, temperature can be measured very comfortably in any direction even from narrow places. In the standard mode of measurement, the temperature can be recorded and stored on an SD card. However, for the online mode, real-time image transfer with a frame rate of 7.5 Hz can be measured and transferred to the attached computer. While taking images, the camera was placed at about 30 cm distance from the surface of the specimen. Ambient temperature and relative humidity of the testing room were measured at the start of the tensile test for each specimen and these values were provided to the input of the thermography camera. The camera is also accessed with an automatic emissivity correction factor. As the original surface of the specimen had a very low emissivity due to this, it can act as a mirror and can cause problems in the testing procedure. The most common and feasible technique is to cover the surface of the inspected specimen by using a flat paint of high emissivity of around 0.90 [16], [17]. For the current research, to avoid the difficulties due to emissivity, a thin layer of black paint having an emissivity of 0.94 was sprayed at the gauge length of the specimen.

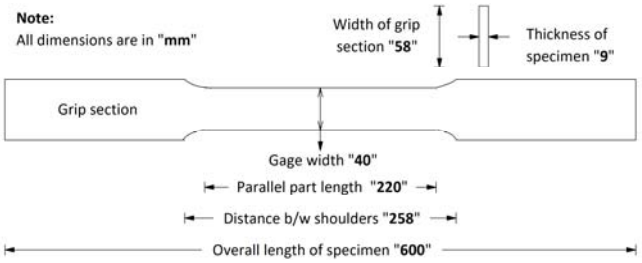

Fig. 2 Dimensions and geometry of the tested specimen

D. Experimental Data Analysis

To validate the results obtained from the thermography technique, three post-yield strain gauges were placed at the gauge length of the specimen. The conventional method of plotting the stress-strain curve and detecting the yield point by taking the assumed value of 0.2% plastic strain was used. The yield point was detected by thermographic technique using the basic concept of thermoelastic effect. The thermoelastic effect reflects the relation between four quantities that are, temperature, entropy, stress, and strain. The temperature change due to tensile loading in the elastic region can be expressed by (1) developed by Lord Kelvin [18]. In this relation, α represents the linear thermal expansion coefficient, T is the initial absolute temperature, c_σ shows the heat capacity per unit volume at constant stress and $\Delta\sigma_s$ represents the change of stress. For quantities $(\Delta T, \Delta\sigma)$ involved in (1), the subscript "s" is the entropy generally known as the degree of randomness in the system [19].

$$\Delta T_S = -\alpha \left(\frac{T\Delta\sigma_s}{c_\sigma}\right) \quad (1)$$

During deformation, a fraction of mechanical energy consumed in plastic deformation is dissipated in the form of heat, approaching to a state when the temperature of the strained specimen starts to rise. The macroscopic plastic deformation within the specimen becomes dominant at this stage. It is interesting to note that, a material with positive α value such as steel, tested under tensile loading, initially exhibits a decrease in temperature, reaches a minimum value, and finally the temperature of the specimen will increase exponentially [20]. In the present research, the yield point has been determined by using this whole concept of thermomechanical coupling as the minimum value of temperature will correspond to the yield point.

E. Numerical Analysis

To check the authenticity of the data obtained from experiments, a fully coupled temperature displacement analysis was performed using Abaqus/Standard. Usually, this analysis is performed when the thermal (temperature distribution) and mechanical (displacement or stress) solutions depend strongly on each other and need to be analyzed simultaneously [21]. For precise analysis, the value of maximum allowable temperature change at each increment $(\Delta\theta_{max})$ was set to be as 0.5 °C. For the sake of meticulous analysis, the analytical model was divided into several parts so that proper mesh size can be given to each part according to the required level. To explain the meshing details in a better manner, a 2D analytical model with the labeling of different parts and zoomed view of meshing has been shown in Fig. 3.

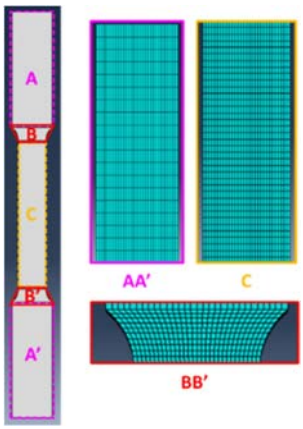

Fig. 3 Meshing details with the help of a 2D analytical model

III. Results and Discussion

A. Disturbance Effect

By examining the thermograms obtained through the

thermography camera, it was found that the temperature profiles of different points showed data scattering. To verify the disturbance effect due to machine operation, temperature imperfections and visible light source, several tests were conducted during the daytime and midnight. All the tests were performed using Thermo FLEX F50 series thermography camera with a frame rate of 7 photos per second. The thermograms were recorded on a PC by setting real-time image transfer mode on the camera. These images were then analyzed using the recording mode of InfReC Analyzer NS9500 Professional for F50 [22].

For testing in the daytime, two specimens of the same dimensions named specimen 1 represented by S1 and specimen 2 characterized by S2, were tested by applying the displacement-controlled loading to check the scattering of data obtained by the thermography technique. An extension of 11 mm was applied to the specimens within 100 seconds by maintaining a loading rate of 5×10^{-4} mm/sec. The ambient temperature recorded for the specimens S1 and S2 at the time of loading was 19.1 °C and 19.6 °C with a relative humidity of 71% and 73% respectively. These tests were performed in the early evening for the time zone between 16:00-18:00 with the presence of visible light in the testing room. Another specimen named specimen 3 denoted by S3 having the same dimensions and loading rate as S1 and S2 were tested at midnight (around 02:00) because at that time almost constant atmospheric conditions prevails as compared to the daytime. The ambient temperature and relative humidity before applying the tensile loading to S3 were measured which comes out to be 21 °C and 64% respectively. For real-time image transfer, it was required to set the target point on the specimen before start of the test. Fig. 4 shows the position of target points for S1, S2 and S3. To make the homogeneity for comparison purpose, efforts were made to focus the similar point for all cases.

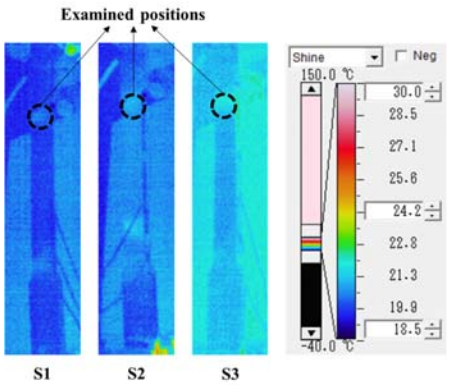

Fig. 4 Location of target points for S1, S2, and S3

To check the disturbance effect due to the presence of visible light source, all the lights in the testing room were turned off during the entire testing activity. To check the disturbance due to the machine operation, photos were recorded 20 seconds before start of the test. All these images recorded under different conditions were analyzed and the temperature profiles have been shown in Fig. 5. It can be seen that the data are showing a similar distribution tested under different conditions.

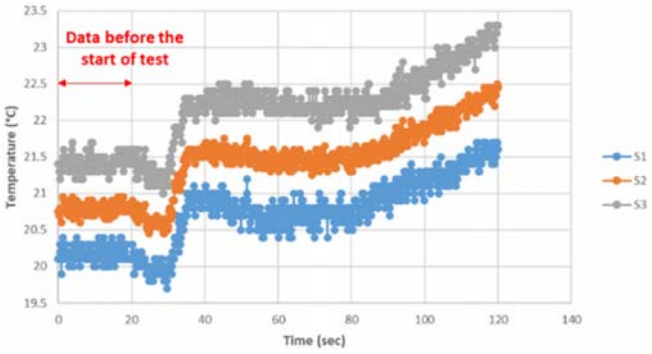

Fig. 5 Temperature profiles for different conditions

The quantitative estimation of disturbance effect was measured in terms of SNR. For image processing, SNR is the ratio of signal mean value (μ) to standard deviation (σ) of signal as represented in (2) [23]:

$$SNR = {}^{\mu}/_{\sigma} \quad (2)$$

Table I shows the results of SNR based on environmental conditions, the time of testing, and the movement of machine. As the value of SNR for all the specimens is almost the same so it can be concluded that the IR thermography camera's performance is independent of testing time and the presence of a visible light source. Moreover, the SNR values calculated for first 20 seconds and for entire test shows similar results depicting that machine operation has no effect on the performance of thermographic camera.

TABLE I
SNR VALUES UNDER DIFFERENT CONDITIONS

Testing conditions	Unit	Specimen 1 (S1)	Specimen 2 (S2)	Specimen 3 (S3)
Time	(hh:mm)	16:40	17:30	02:00
Ambient temperature	(°C)	19.1	19.6	21.0
Relative humidity	(%)	71	73	64
Visible light	-	Present	Present	Nil
SNR (20 seconds)	dB	46.49	46.82	45.92
SNR (entire test)	dB	45.98	45.21	45.03

B. Data Denoising

The temperature profile obtained through the thermography camera was denoised by using the application of wavelet signal denoiser in MATLAB by setting the denoising method and threshold rule as Bayes and Soft, respectively. Level dependent technique was chosen for the noise estimation. Different wavelet types with their respected noise reduction number can be selected to denoise the data, however, an appropriate value for all the factors was selected to denoise the temperature profile data so that the data cannot lose its originality and trend.

As the testing conditions were not same for different specimens, therefore, to get a better understanding of changes in temperature with respect to time, the data were initialized. Fig. 6 shows the denoised and initialized temperature profiles for all the above-mentioned specimens. The changes observed

in temperature profiles between 30 seconds and 40 seconds can be attributed to the denoising of data.

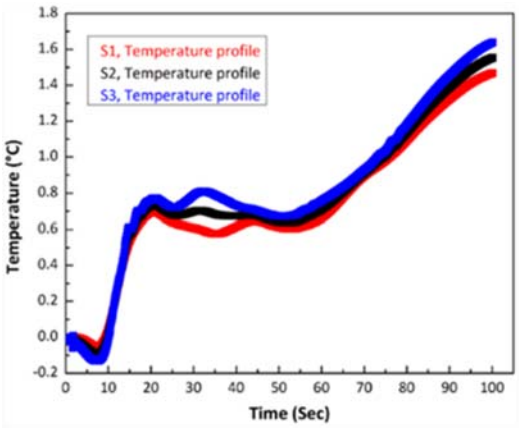

Fig. 6 Representation of denoised and initialized temperature profiles for S1, S2, and S3

C. Yield Point Recognition

By using the thermography technique, yield point of any single point can be determined easily in contrast to the stress-strain curve data which only show the global yield point. In the elastic region, the temperature of the specimen decreases quasi-linearly with the increase of elastic deformation. The minimum value of temperature shows the end of elastic behavior at some local points of the specimen. These points exhibit the localized yielding initiation resulting from the localized stress concentration. For stress concentrations further than the yielding point, heating occurs and temperature start increasing at those localized points. With the increase of tensile loading, more and more points start yielding ultimately resulting in the global yielding.

To explore the above-mentioned phenomena, a coupon specimen was tested and the thermograms have been shown in Fig. 7. It can be seen that at the start of the test, the color of the specimen is lighter showing the ambient temperature expressed in Fig. 7 (a). With the increase in tensile loading, the specimen color becomes darker showing the drop in temperature just before yielding as shown in Fig. 7 (b). Finally, the thermogram represented in Fig. 7 (c) represents the localized yielding initiation of the specimen in which the color shows a higher value of temperature highlighted with circles.

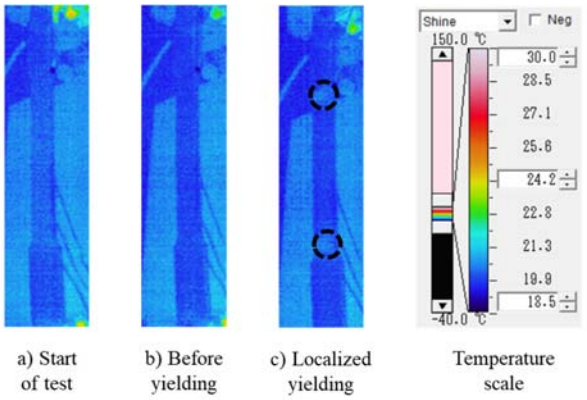

Fig. 7 Thermoelastic effect definition by thermograms captured by IR thermography camera

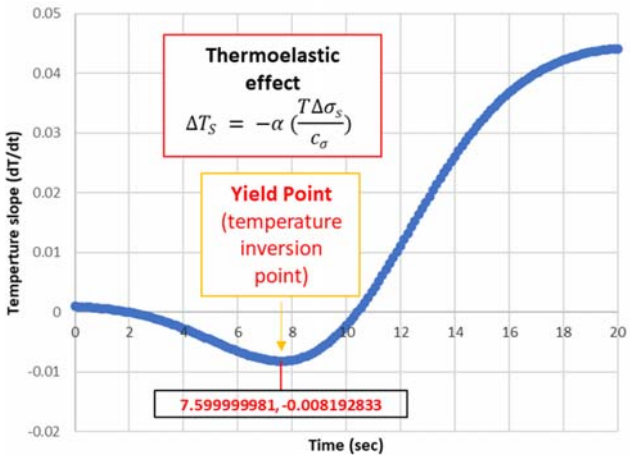

Fig. 8 Temperature slope representing the yield point

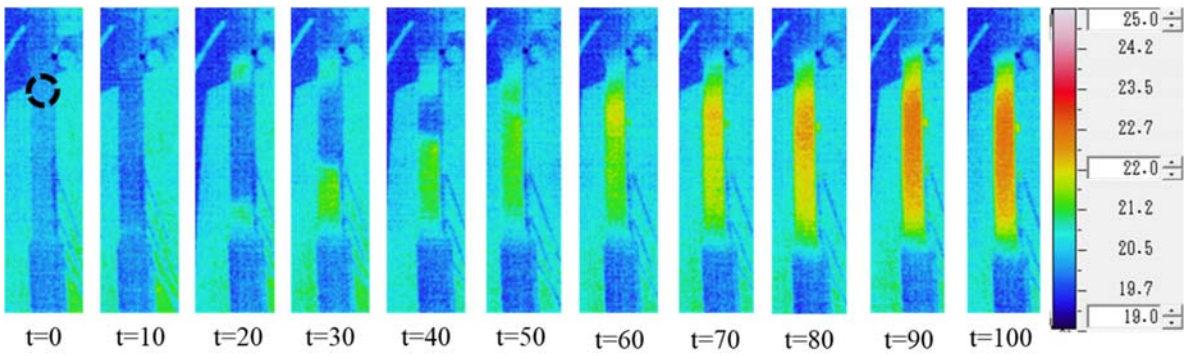

Fig. 9 Heat generation mechanism due to the applied loading

The phenomenon in which elastic deformation of an object in adiabatic conditions is always be associated with the temperature change is called the thermoelastic effect first explored by W. Thomas (Lord Kelvin) [18]. The temperature inversion point, at which the temperature slope changes from negative to positive, indicates the transition from thermoelastic to plastic behavior, the yield point. In Fig. 8, approximately at 7.6 seconds the temperature slope represents the yield point. In

order to clearly indicate the yield point on the curve, only 1/5th of the data set has been shown in Fig. 8. Fig. 9 shows the heat generation mechanism within the specimen due to the applied loading with respect to time (t) in seconds. When load starts increasing, the generation of heat begins due to the localized yielding at the notched parts of the specimen and spreads over larger area with the passage of time. The prime purpose of this study is to focus the yielding initiation point (represented by a black circle in the thermogram at t equals to 0 seconds). This is important because in structural steel members when the yielding occurs locally, the plastic strain changes the fracture toughness and even the yield point itself and hence changes the material properties. Local yield point or the point where yielding initiates within a member is very important as the local cyclic loading causes the fatigue cracking and sometimes the brittle fracture.

D. Validation of Thermography Technique

For validation purpose, the temperature profile was compared with the stress-strain curve as well as the analytical results obtained from Abaqus. In order to overcome the effect of initial imperfections for the analytical results, pre-strained specimen was used for testing. Another purpose of pre-straining was to illustrate the behavior for cyclic loading. During the pre-straining of specimen, an extension of 11 mm was applied for 100 seconds, then the specimen was unloaded to 0 kN and after that, again loaded for 11 mm displacement within 100 seconds.

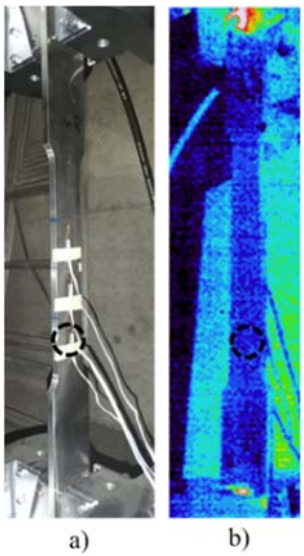

Fig. 10 Target point for the formation of the stress-strain curve and corresponding temperature profile

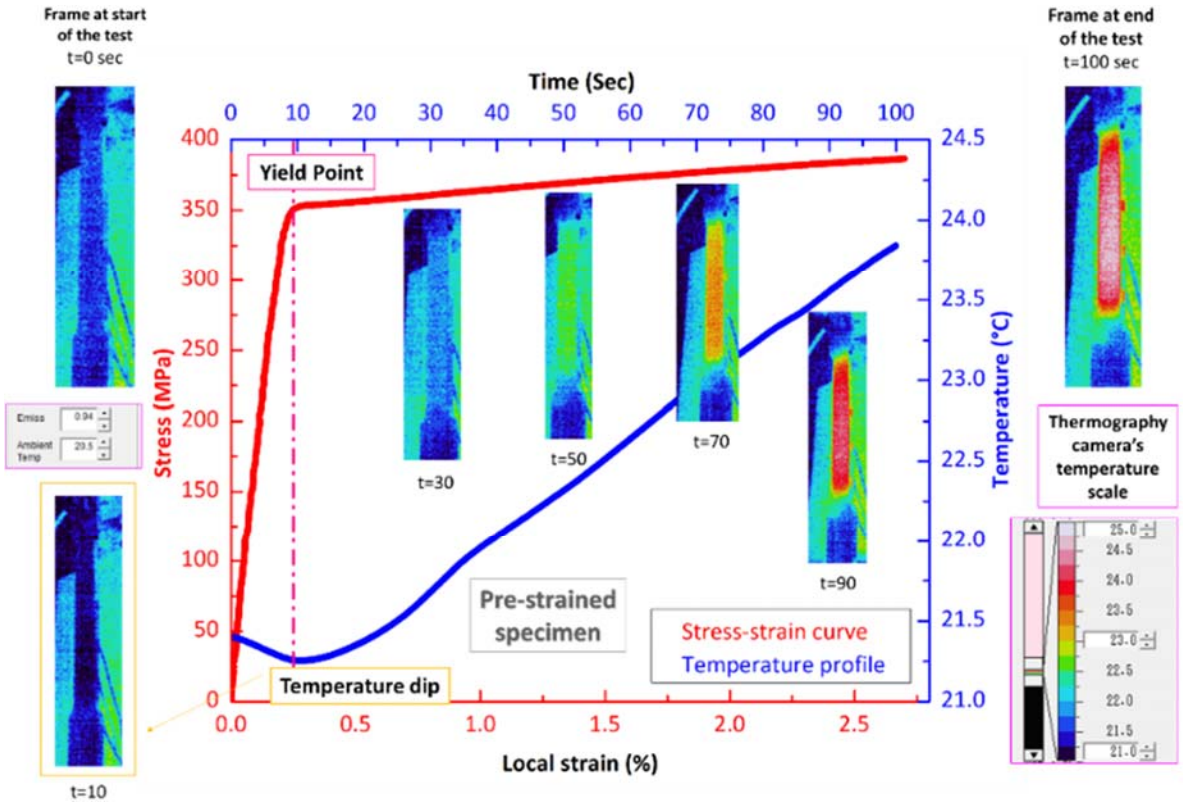

Fig. 11 Stress-strain curve vs. temperature-time profile

1. Stress-Strain Curve vs. Temperature Profile

The target point for the formation of the stress-strain curve and temperature profile is the point where the bottom strain gauge was glued to the specimen as depicted in Fig. 10. The stress-strain curve obtained from the loading/unloading data is plotted against the temperature profile which is the evolution of heat w.r.t time as represented in Fig. 11. The thermograms on this graph show the distribution of temperature at different time

intervals. The important thermogram is at t = 10 sec because it shows the decrease in temperature as compared to the frame at the t = 0 showing the position of yield point. This decrease in temperature clearly can be seen through the temperature dip appeared in the temperature profile. The yield point shown through stress-strain curve is found to be exactly same as indicated by the temperature dip.

The results of yield point detection in the pre-strained specimen revealed that for structural steels the IR thermography method can be utilized for the cycling loading experiments. Also, for a pre-strained specimen in which the stress-strain curve does not provide with a clear yield point, a vivid yield point can be determined by temperature dip from the thermography camera. As the same phenomena occurs during the testing of high strength steel, the result from pre-strained specimen shows the feasibility of extension of the thermography technique for high strength steel too.

2. Experimental vs. Analytical Results

The experimental temperature profile was compared with the analytical results at the target point within the specimen as represented in Fig. 12. The comparison between the results from numerical simulation and the experimental temperature profile is illustrated in Fig. 13. It is remarkable to note that, for numerical simulation, no temperature inversion will take place because it happens due to the adiabatic environment in the testing procedure. However, during analysis, the yield point can be identified by the increase in temperature. Before yielding, the temperature increase will be zero; but with the initiation of localized yielding, the temperature increment can be seen due to the plastic deformation. The stress profile (nominal stress with respect to time) is also drawn with the experimental and analytical temperature profiles, showing delay in yield point as it provides globalized yielding. The temperature distributions from coupled thermal displacement analysis and the IR thermography camera are almost the same hence, showing a good correlation between numerical analysis and experimentation by implementing the thermography technique.

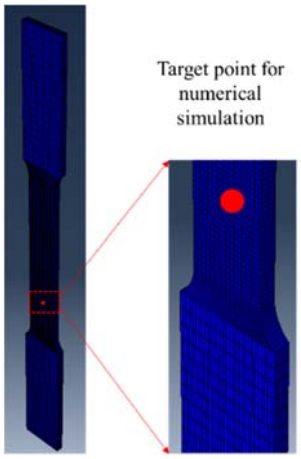

Fig. 12 Target point for numerical simulation for comparison with the experimental results

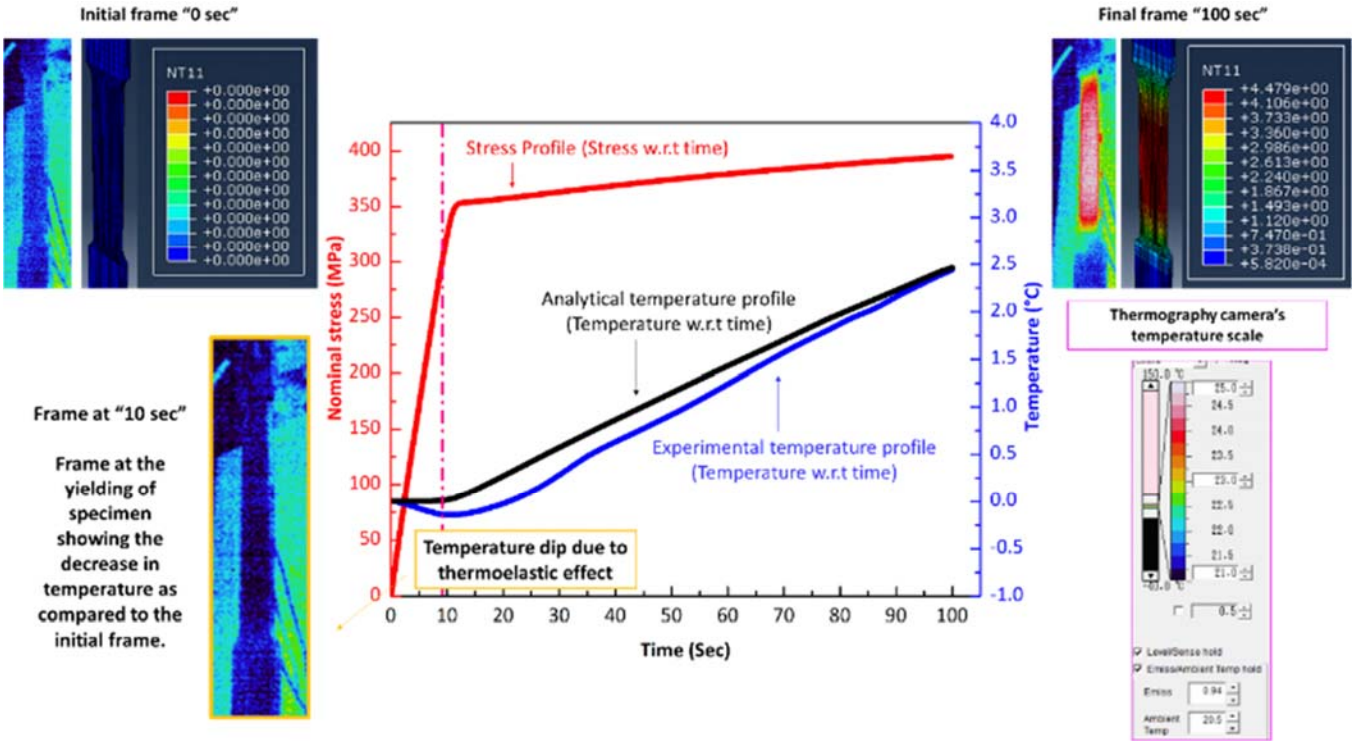

Fig. 13 Comparison of experimental and analytical temperature profiles

It can be unveiled from Fig. 13 that the stress profile which was obtained by the applied load from the loading machine, the initial yielding point cannot be judged at a particular position. In other words, the load profile (load curve with respect to time)

is unable to provide the identification of local yield point whereas the IR thermography technique can detect the yield point locally at any position within a specimen and also the point where the yielding initiates.

IV. Conclusion

Identification of localized yield point is very important as the local cyclic loading causes the fatigue cracking and sometimes the brittle fracture. By using the thermography technique, yield point determination of every single point can be performed easily which is difficult by using the stress-strain curve data because it provides the global yield point in tensile testing. Detection of yield point initiation by using the IR thermographic technique is showing good correlation with the conventional method as well as with the numerical analysis which proves that the infrared thermography technique can be used for the precise recognition of yield point in structural steel specimens. This accurate temperature-based detection technique can be extended to real complex shaped structural steel members. In case of complicated geometry members, by using strain gauge method lots of effort will be required for testing with relatively more chances of mistake. Those problems can be overcome by employing the IR thermography technique.

References

[1] R. Hill, "LXXXVIII. On the state of stress in a plastic-rigid body at the yield point," *London, Edinburgh, Dublin Philos. Mag. J. Sci.*, vol. 42, no. 331, pp. 868–875, 1951.

[2] T. Burczyński, W. Beluch, A. Dlugosz, W. Kuś, M. Nowakowski, and P. Orantek, "Evolutionary computation in optimization and identification," *Comput. Assist. Mech. Eng. Sci.*, vol. 9, no. 1, pp. 3–20, 2002.

[3] A. Rogalski, *Infrared detectors*. 2009. doi: 10.1142/9789812834133_0014.

[4] B. M. Gratt and M. Anbar, "Thermology and Facial Telethermography: Part II. Current and Future Clinical Applications in Dentistry," *Dentomaxillofacial Radiol.*, pp. 68–74, 1998.

[5] L. Chaerle, W. V. Caeneghem, E. Messens, H. Lambers, M. V. Montagu, and D. V. D. Straeten, "Presymptomatic Visualization of Plant-Virus Interactions by Thermography," *Nat. Biotechnol.*, pp. 813–816, 1999.

[6] D. S. P. Rao, "Infrared thermography and its applications in civil engineering," *Indian Concr. J.*, vol. 82, no. 5, pp. 41–50, 2008.

[7] S. R. Khedkar and P. V. R. Dhawale, "Infrared Thermography and Its Application in Building," no. May, pp. 57–61, 2019.

[8] I. Todhunter and K. Pearson, *A History of the Elasticity and Strength of Materials*, Vol. 2. Cambridge University Press, 1893.

[9] M. A. Biot, "Thermoelasticity and Irreversible Thermodynamics," *J. Appl. Phys.*, pp. 240–253, 1956.

[10] H. Sakamoto, I. Oda, T. Doi, and M. Yamamoto, "Evaluation system of plastic deformation in elasto visco-plastic body with crack by infrared thermography," *Trans. Eng. Sci.*, vol. 6, pp. 453–459, 1994.

[11] H. Sakamoto, "Estimation of plastic deformation in strain rate dependence materials by infrared video system," *Trans. Model. Simul.*, vol. 16, pp. 67–76, 1997.

[12] B. Venkataraman, B. Raj, and C. K. Mukhopadhyay, "Characterisation_of_Tensile_Deformation_through_Infrared_Imaging_Technique.pdf," *J. Korean Soc. Nondestruct. Test.*, vol. 22, 2002.

[13] A. Lipski, "Impact of the strain rate during tension test on 46Cr1 steel temperature change," *Key Eng. Mater.*, vol. 598, pp. 133–140, 2014, doi: 10.4028/www.scientific.net/KEM.598.133.

[14] B. Venkatraman, M. Menaka, and B. Raj, "Thermography for Characterisation of Deformation Process in Stainless Steels," no. January 2017, 2014, doi: 10.21611/qirt.2014.165.

[15] E. Stange, Z. Andleeb, H. Khawaja, and M. Moatamedi, "Multiphysics study of tensile testing using infrared thermography," *Int. J. Multiphys.*, vol. 13, no. 2, pp. 191–202, 2019, doi: 10.21152/1750-9548.13.2.191.

[16] M. Kutin, S. Ristić, Z. Burzić, and M. Puharić, "Testing the Tensile Features of Steel Specimens by Thermography and Conventional Methods," vol. 60, no. 1, pp. 66–70, 2010.

[17] M. M. Kutin, S. S. Risti, M. R. Prvulovi, M. M. Prokolab, N. M. Markovi, and M. R. Radosavljevi, "Application of thermography during tensile testing of butt welded joints," *FME Trans.*, vol. 39, no. 3, pp. 133–138, 2011.

[18] Lord Kelvin, *Trans. Roy. Soc.* Edinburgh, 1853.

[19] W. Oliferuk, A. Korbel, and M. W. Grabski, "Slip behaviour and energy storage process during uniaxial deformation of austenitic steel tensile," vol. 236, pp. 1122–1125, 1997.

[20] R. Rocca and M. B. Bever, "the Thermoelastic Effect in Iron and Nickle as a function of temperature," vol. 188, no. 1830, pp. 327–333, 1950.

[21] M. Smith, *ABAQUS Analysis User's Guide, Version 6.14*. Dassault Systèmes Simulia Corp, 2014.

[22] N. Avionics, "InfReC Analyzer NS9500 Professional for F50 (User Manual)." 2017.

[23] D. R. Parrish, Todd B.Gitelman, K. S. LaBar, and M. M. Mesulam, "Impact of signal-to-noise on functional MRI," *Magn. Reson. Med.*, vol. 12, no. 16, pp. 925–932, 2000, doi: 10.1097/00001756-200111160-00017.